

Chapter 6

Journal of Applied Electrochemistry
<https://doi.org/10.1007/s10800-025-02278-1>

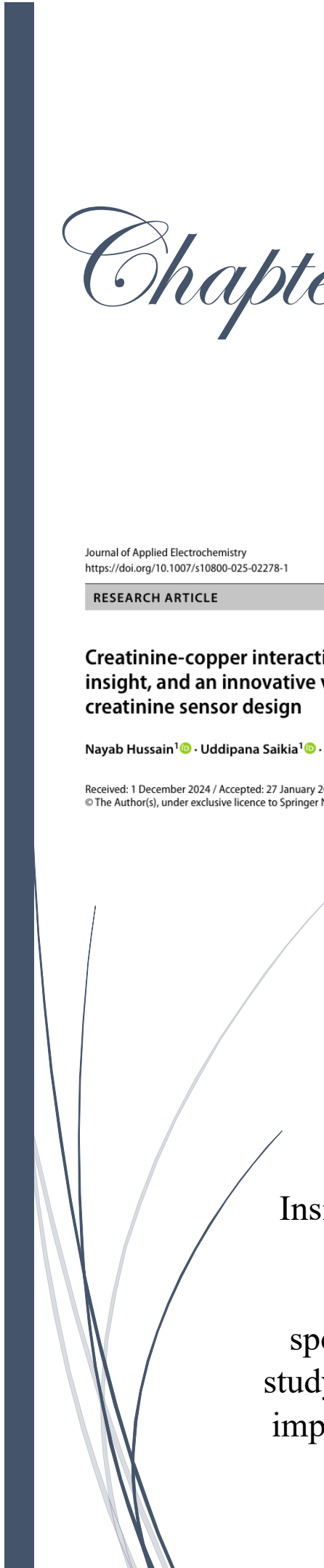
RESEARCH ARTICLE



Creatinine-copper interaction: electrochemical and spectroscopic insight, and an innovative verification of a molecularly imprinted creatinine sensor design

Nayab Hussain¹ · Uddipana Saikia¹ · Panchanan Puzari¹

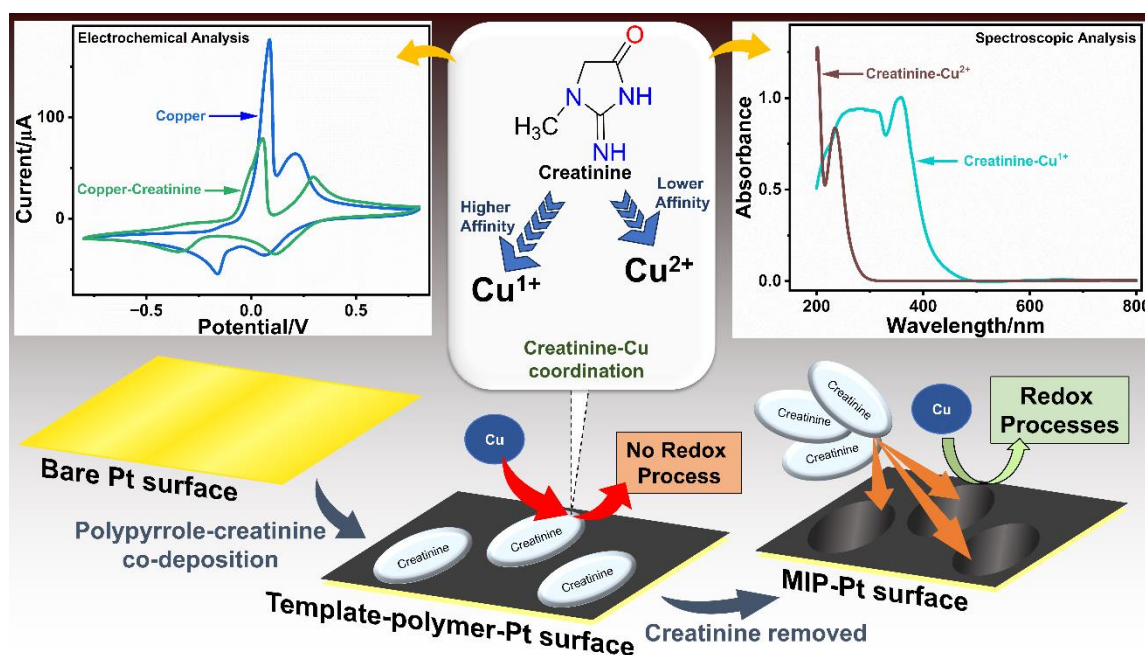
Received: 1 December 2024 / Accepted: 27 January 2025
© The Author(s), under exclusive licence to Springer Nature B.V. 2025



Insight into the creatinine-copper interaction through electrochemical, UV-vis spectrometric and impedimetric study and feasibility of molecularly imprinted creatinine sensor design

Highlights

This chapter deals with the electrochemical characterization of copper and distinguishes its electrochemical response with well-resolved redox peaks by studying the effect of the initial forward potential sweep direction. Noting the changes in the redox processes of copper in the presence of creatinine, the copper-creatinine interaction was studied so as to ascertain the oxidation state of copper, the creatinine molecules interact with solely or preferentially. The creatinine-copper electrochemical analyses were carried out with both bare Pt electrode and Cu⁰-deposited Pt electrode. UV-vis analysis of the interaction between creatinine and copper ions is also presented. Furthermore, the electrochemical fabrication of Pt electrode decorated with creatinine-imprinted-polypyrrole is demonstrated. The creatinine-copper interaction has been utilized to confirm the fabrication of the creatinine-sensing platform. SEM images of the electrode materials are also analyzed. CV, DPV and EIS techniques are used for the electrochemical analyses. CA and CP techniques are employed for electrode modifications.



This part of the thesis is published as:

Hussain, N., Saikia, U. and Puzari, P. Creatinine-copper interaction: electrochemical and spectroscopic insight, and an innovative verification of a molecularly imprinted creatinine sensor design. *Journal of Applied Electrochemistry*, 2025. DOI: <https://doi.org/10.1007/s10800-025-02278-1>

6.1 Introduction

The changes in the native redox peaks of copper in the presence of creatinine have been explored several times to develop electrochemical creatinine determination methods [1-4]. While *Raveendran et al.* [1], *Sato et al.* [2] and *Jankhunthod et al.* [3] used copper-deposited electrodes to record the voltammograms of buffer or electrolyte solutions in the absence and presence of creatinine, *Kaewket and Ngamchuea* [4] reported the use of a bare Pt macrodisk electrode to record the voltammogram of creatinine solution in the absence and presence of Cu^{2+} ions. In such work, the voltammogram exhibiting the redox peaks of copper is touted as the reference in which the changes by adding creatinine are noted.

It can be comprehended that the electrochemical response of copper can be obtained by either recording voltammograms of solutions containing copper ions with bare electrodes or by recording the voltammogram of buffer/electrolyte solutions with Cu^0 deposited electrodes. However, some interesting differences were marked in the reported voltammograms that exhibit only the copper redox peaks. While in the voltammogram presented by *Sato et al.* [2], only one pair of redox peaks was observed for copper, two distinct reduction peaks along with multiple seemingly unresolved oxidation peaks were observed in the voltammogram presented by *Raveendran et al.* [1]. On the other hand, *Jankhunthod et al.* [3] reported a voltammogram which showed two well-resolved oxidation peaks, but only one reduction peak in the selected potential window. Only one pair of redox peaks was also observed in the voltammogram reported by *Kaewket and Ngamchuea* [4] for an electrolyte solution containing Cu^{2+} ions. The difference in the shapes and resolution of the voltammograms can be attributed to factors like the type of working electrode, the resolution power of the workstation, the concentration of the copper ions and the oxidation state at which copper is dominantly present at the beginning of the voltammogram runs. However, one factor that can alter the electrochemical response of copper, which has never been studied earlier, is the initial forward potential sweep direction.

Moreover, some differences were also noted in the trend of the changes that occur in the electrochemical response of copper due to the presence of creatinine, which raises some ambiguity. *Raveendran et al.* [1] and *Sato et al.* [2] reported similar observations that the intensity of the oxidation peaks of copper increases, while that of reduction peaks

decreases in the presence of creatinine. However, the reverse was reported by *Jankhunthod et al.* [3]. Studying the interaction between creatinine and Cu^{2+} ions in aqueous medium with a bare electrode, *Kaewket and Ngamchuea* [4] reported the inhibition of both redox peaks of copper in the presence of creatinine. Although no common trend in the voltammogram changes was reported, both positive and negative changes in the intensity of copper redox peaks were unanimously attributed to the well-established coordination of creatinine with Cu^{2+} ions [5-7]. Creatinine can act as a monodentate ligand by coordinating with Cu^{2+} ions via its cyclic nitrogen atom and a bidentate ligand by coordinating via the cyclic nitrogen atom and the oxygen atom of the carbonyl group [6].

At this point, it is important to note that evidence of creatinine coordination with Cu^{1+} ions has also been reported recently [8]. In most electrochemical creatinine determination methods based on creatinine-copper interaction, the prime objective is to establish a linear change in the intensity of the redox peaks of copper with creatinine concentration. Thus, the correct assignment of the redox process which is affected by the presence of creatinine or the oxidation state(s) of copper with which the creatinine coordination occurs, is not often in focus. However, to understand the precise mechanism of creatinine-copper interaction during the voltammogram runs, it is important to establish the conditions at which stable and reproducible electrochemical response of copper can be obtained, with well-resolved redox peaks.

Furthermore, regardless of copper being initially present as Cu^{2+} ions in the solution or as Cu^0 deposited on the electrode surface, Cu^+ ions are also produced during the voltammogram runs. Considering the ability of creatinine coordination with not just Cu^{2+} ions but also with Cu^+ during the electrochemical processes, alternative explanations may be provided for the changes in the electrochemical response of copper due to the presence of creatinine. Hence, this chapter focuses on establishing a stable and well-resolved electrochemical response of copper by studying the influence of the initial forward potential sweep direction and correct interaction between creatinine and copper. A study of creatinine-copper interaction from a spectroscopic perspective and detailed electrochemical characterization of copper has also been presented. This study is aimed to address the ambiguities mentioned above.

Another objective of this work is the electrochemical preparation of an MIP-based sensing platform for creatinine. As MIP-based techniques have also found prominence in the sensitive determination of creatinine, it is noted that most of the reported sensing platforms are prepared by drop-coating the materials on the electrode surface [9-11]. A benefit of the drop-coating method is that the sensing materials can be carefully removed from the surface and characterized to verify the formation of the MIP platform, by electron microscopy or spectroscopic techniques. The material characterization can also be accomplished before deposition in some cases. However, precise controls are required over the homogeneity, thickness, volume and mass of the sensing materials that are drop-coated on the electrode surface, to get accurately reproducible electrochemical responses. These factors can be easily controlled in electrochemical deposition techniques by fixing the electrochemical parameters. So, in this chapter, we have also demonstrated that an MIP-based creatinine sensing platform can be successfully fabricated using the electrodeposited polypyrrole matrix.

Thus, to sum up, this chapter focuses on exploring the creatinine-copper interaction from electrochemical and spectroscopic perspectives. The electrochemical responses are recorded for a) solutions containing creatinine and copper ions with bare Pt electrode, and b) buffer containing creatinine with Cu^0 deposited Pt electrode. UV-vis spectroscopy is employed to study creatinine- Cu^{2+} interaction. Furthermore, a unique approach has also been presented to validate the formation of the MIP sensing platform by utilizing the creatinine-copper interaction. The work has created a new avenue for copper metal-based creatinine sensor development.

6.2 Experimental

6.2.1 Chemicals, reagents and instruments

Copper sulphate pentahydrate, potassium chloride, acetonitrile and sulphuric acid were procured from Merk; creatinine (98%) from Alfa Aesar; pyrrole and cuprous iodide from Sigma-Aldrich; dipotassium hydrogen phosphate from SRL; potassium dihydrogen phosphate and potassium nitrate from Rankem. All these chemicals were of analytical grade and were used without further purification. Phosphate buffer saline (PBS) of 0.1 M strength was used.

Biologic SP-300 (EC-Lab software setup) was used for electrochemical analyses. UV-2600I (Shimadzu) was used to record the UV-vis spectra and PerkinElmer FTIR spectrophotometer was used to record the FTIR spectra. SEM images were obtained with JSM 6390LV (JEOL, Japan).

6.2.2 Electrochemical studies with bare electrode

Electrochemical responses of copper were studied by recording CVs of aqueous $\text{CuSO}_4 \cdot 5\text{H}_2\text{O}$ solutions in the presence of 0.1 M KCl as a supporting electrolyte. As in the potentiostatic electrochemical impedance spectroscopy technique (PEIS), the sinusoidal alternating voltage is superimposed over a DC voltage, the $\text{CuSO}_4 \cdot 5\text{H}_2\text{O}$ solution was also electrochemically characterized with the PEIS technique by determining the DC voltage at which the kinetics of the redox transfer is the quickest. Furthermore, CVs were also recorded for the $\text{CuSO}_4 \cdot 5\text{H}_2\text{O}$ solutions spiked with different concentrations of creatinine, to study the creatinine-copper interaction in the aqueous medium.

The CVs were recorded in the potential window of -0.8 V to 0.8 V and a scan rate of 50 mV s^{-1} . The PEIS responses were recorded in the 1 MHz – 100 MHz frequency range, with a sinus amplitude of 10 mV . All these electrochemical analyses were carried out with a well-polished bare Platinum (Pt) working electrode, Ag/AgCl/KCl (3.5 M) reference electrode and Ag wire as a counter electrode.

6.2.3 Electrode modifications and electrochemical studies

6.2.3.1 Cu^0/Pt electrode

Cu^0/Pt electrode was prepared by electrochemically depositing Cu^0 on the surface of Pt electrode. With a Platinum (Pt) working electrode, Ag/AgCl/KCl (3.5 M) reference electrode and Ag wire as a counter electrode, the chronoamperometry (CA) technique was employed to modify the electrode surface, as reported in the literature [2]. Accordingly, an acidic solution of $\text{CuSO}_4 \cdot 5\text{H}_2\text{O}$ (1 mM) was prepared in 0.01 M H_2SO_4 and taken in the electrochemical cell. Then, CA was employed to accomplish the electrochemical deposition. The CA response was recorded by holding the potential at 0.3 V for 10 s and then, stepping it to -0.2 V at which the system is maintained for 200 s .

The modified electrode was used to record the CV and DPV responses of PBS (pH 7.4) and 1 mM creatinine solution (CRS) prepared in the PBS. Thus, the electrochemical

response of creatinine with the Cu^0/Pt electrode was studied. The CVs were recorded in the potential window of -0.7 V to 0.7 V and a scan rate of 50 mV s^{-1} . The DPVs were recorded in the potential window of -0.15 V to 0.7 V , with 2.5 mV pulse height, 100 ms pulse width, 5.0 mV step height, and 500.0 ms step time.

6.2.3.2 MIP electrode

The surface of the Pt electrode was modified with a creatinine-imprinted polypyrrole (CIP) matrix to yield the CIP/Pt electrode. The fabrication was accomplished by chronopotentiometry (CP) technique. A solution of 0.1 M KNO_3 containing 100 mM pyrrole monomer and 30 mM creatinine molecule was prepared and taken in the electrochemical cell. Using a Platinum (Pt) working electrode, $\text{Ag}/\text{AgCl}/\text{KCl}$ (3.5 M) reference electrode and Ag wire as a counter electrode, the CP technique was employed at the constant current of $1\text{ mA}/\text{cm}^2$ for 400 seconds, to fabricate the electrode surface with Template Impregnated Polymer (TIP), containing co-deposited creatinine and polypyrrole (PPy). Then the modified electrode surface was dipped into distilled water and washed with continuous stirring to dissolve the creatinine molecules from the electrode surface. The electrode surface was then dried at $50\text{ }^\circ\text{C}$ to prepare the CIP/Pt electrode.

CP was also employed for 0.1 M KNO_3 solution containing only 100 mM pyrrole monomer to fabricate the Pt electrode with PPy, which is a well-established method in the literature [12]. The difference in the CP responses for deposition of PPy and co-deposition of PPy and creatinine was noted.

CVs were recorded for $5\text{ mM CuSO}_4\cdot 5\text{H}_2\text{O}$ solution prepared with 0.1 M KCl as the supporting electrolyte, with CIP/Pt and TIP/Pt electrode, in the potential window of -0.45 V to 0.55 V , with a scan rate of 50 mV s^{-1} . The successful fabrication of the CIP/Pt electrode was proven by comparing the voltammograms. Further evidence was gathered by recording galvanostatic electrochemical impedance spectroscopy (GEIS) for CRS containing different creatinine concentrations. The GEIS responses were recorded in the frequency range of 5.00 MHz to 500 Hz , with an amplitude of $100.00\text{ }\mu\text{A}$.

6.2.4 Spectroscopic analysis

Creatinine-copper interaction was analyzed with UV-vis spectroscopy. To study the creatinine interaction with Cu^{2+} ions, separate UV-vis spectra of a $0.1\text{ mM CuSO}_4\cdot 5\text{H}_2\text{O}$

solution, a 0.1 mM CRS and a mixture of both maintaining the same molarity were recorded in PBS (pH = 7.4). To study the creatinine interaction with Cu^{1+} ions, separate UV-vis spectra of 5 mM CuI solution, a 5 mM CRS and a mixture of both maintaining the same molarity were recorded in 1:1 acetonitrile-water medium.

UV-vis and FTIR spectroscopy were further employed to study the interaction between creatinine and pyrrole, by separately recording the spectra of a 10 mM pyrrole solution, a 3 mM CRS and a mixture of both maintaining the same molarity, prepared in 0.1 M KNO_3 .

The UV-vis spectra were recorded in the 200–800 nm frequency range and the FTIR spectra were recorded in the 4000–400 cm^{-1} wavenumber range.

6.3 Results and Discussion

6.3.1 Electrochemical response of copper sulphate solution and the influence of the potential sweep direction

CVs of a 10 mM $\text{CuSO}_4 \cdot 5\text{H}_2\text{O}$ solution (with 0.1 M KCl as electrolyte) were recorded by applying the initial forward potential sweep in opposite directions. Figure 6.1 shows the 1st cycles (A) and the 11th cycles (B) of the recorded CVs, corresponding to each sweep direction.

In ‘Cycle-1’, as shown in Figure 6.1 (A), when the forward potential sweep was applied from higher to lower potential (0.8 V to –0.8 V), two reduction peaks (R_1 and R_2) were obtained at first. The two oxidation peaks (Ox_1 and Ox_2) were obtained during the reverse scan. The R_1 and Ox_2 peaks can be assigned to the $\text{Cu}^{2+}/\text{Cu}^{1+}$ redox processes, and the peaks, R_2 and Ox_1 , can be assigned to the $\text{Cu}^{1+}/\text{Cu}^0$ redox processes [13-16].

However, in ‘Cycle-1’, when the forward potential sweep was applied from lower to higher potential (–0.8 V to 0.8 V), only one oxidation peak, Ox_2 , was observed during the forward scan and one reduction peak, R_2 , during the reverse scan. This indicates the dominant presence of Cu^{1+} ion in the system, to satisfy the Nernst equation during the initial application of large negative potentials. The other expected redox peaks (Ox_1 and R_1) were apparently unresolved in the CV, due to the low concentrations (and thus, low

peak intensities) of Cu^{2+} and Cu^0 in the system. This also explains the comparatively broader appearance of the peaks, Ox_2 and R_2 , where the peaks due to the other redox processes stayed masked. All four redox peaks appeared distinctively resolved from the next cycle.

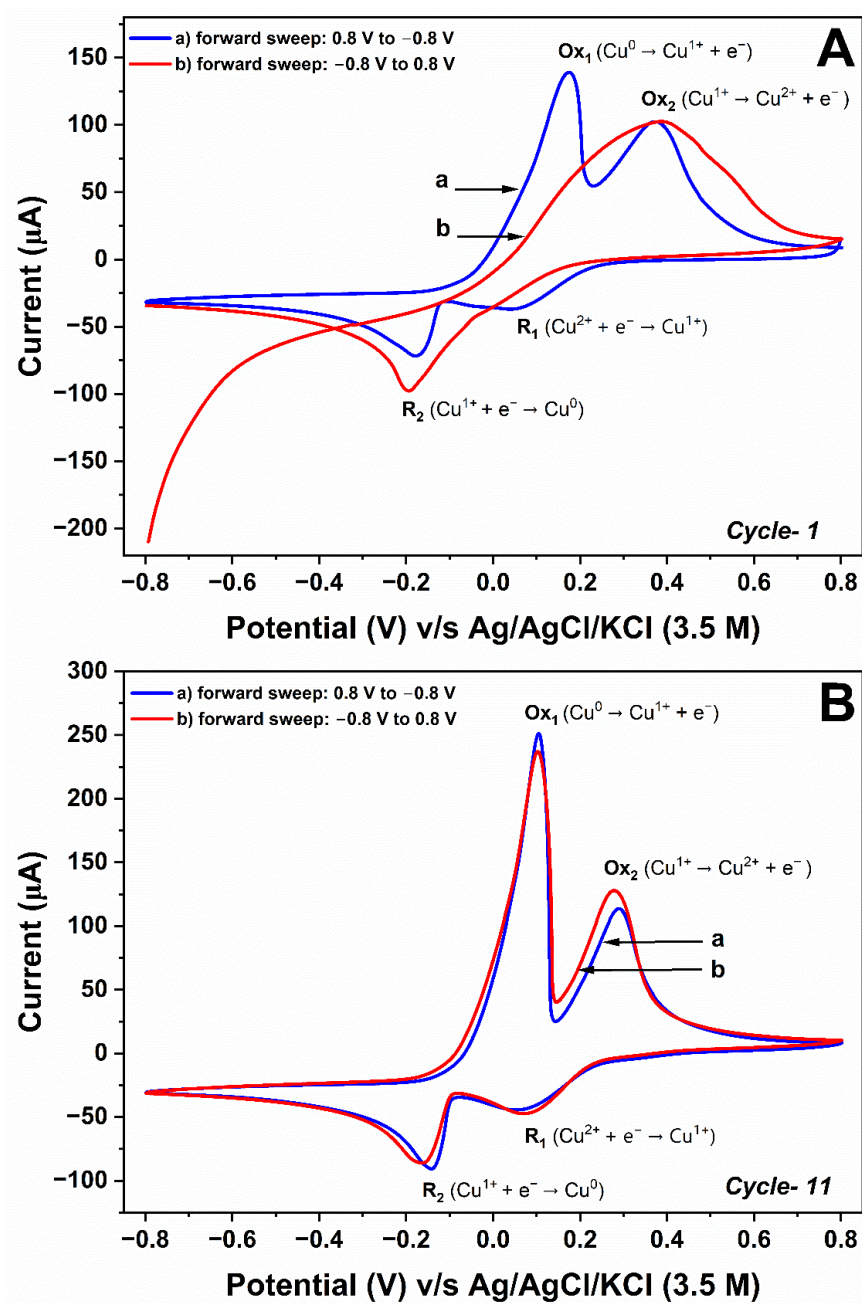


Figure 6.1: 1st cycle (A) and 11th cycle (B) of the CV recorded for copper sulphate solution with the initial forward potential sweep applied from a) 0.8 V to -0.8 V and b) -0.8 V to 0.8 V.

The voltammograms appeared similar when the respective 11th cycles were compared, as can be seen in Figure 6.1 (B). These voltammograms can be touted as stable, where the peak positions and intensities are almost equal, irrespective of the potential sweep direction.

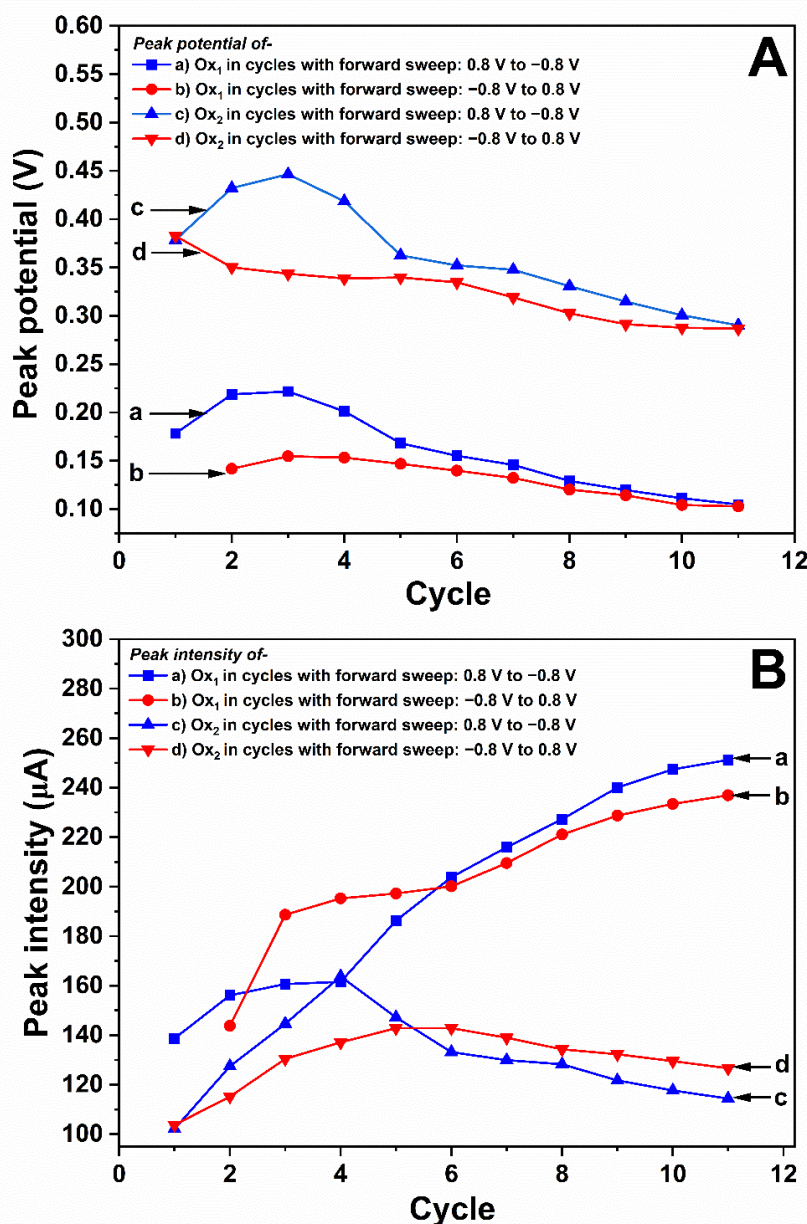


Figure 6.2: Variations of peak potential (A) and intensity (B) of Ox₁ and Ox₂ in cycles with opposite forward potential sweep directions.

Figure 6.2 shows the plots of the potential (A) and the intensity (B) of the oxidation peaks (Ox₁ and Ox₂) against the cycles of the CVs. Differences in the peak potentials

(positions) and intensities were observed during the initial cycles in the plots when the corresponding values were compared for voltammograms with opposite forward potential sweep directions.

Figure 6.2 (A) shows notable differences between the corresponding potentials of Ox₁ till the 4th cycle. Similarly, differences between the corresponding potentials of Ox₂ were also observed till the 4th cycle, although the peak positions in the respective 1st cycle were almost equal. The difference narrowed in both cases, from the 5th cycle and eventually, the potentials for the corresponding peaks became almost equal in the 11th cycle. The positions for both peaks showed a slight overall shift towards lower potentials as the voltammogram cycles proceeded.

Figure 6.2 (B) also shows differences in the corresponding intensities of Ox₁ and Ox₂ in the initial cycles of the voltammograms. The intensities of Ox₁ were noted to be the closest when the 6th cycles were compared, following which the intensities maintained narrow differences in the subsequent cycles. On the other hand, the intensities of Ox₂ were noted to be the closest when the 5th cycles were compared, following which narrow differences were maintained.

It can also be seen that irrespective of the forward potential sweep direction, the intensity of Ox₁ initially increased irregularly with the cycle and eventually tended to attain saturation (expected from the extrapolation of the plots). This indicates the initial increase in the oxidation of Cu⁰ to Cu¹⁺ until an equilibrium in the system is established. The intensities obtained due to the oxidation of Cu¹⁺ to Cu²⁺, represented by Ox₂, were comparatively low. However, similar trends in the intensity variation of Ox₂ with the cycle were also noted, irrespective of the forward potential sweep direction. The intensity of Ox₂ was noted to increase slightly at first and then, gradually decrease as the system moves towards equilibrium.

This observation clearly indicates that the resolution, intensity and position of the redox peaks of copper vary with the initial forward potential sweep direction. However, this effect is limited to the initial few cycles of the voltammogram runs. Hence, it is recommended to elude the initial cycles while electrochemically studying the creatinine-copper interaction, as it is important to have stable and well-resolved redox peaks of copper to avoid any misinterpretation.

6.3.2 PEIS analysis of the copper sulphate solution

From the potential variation plot of Ox_1 with cycles, as represented by curve ‘a’ and curve ‘b’ in Figure 6.2 (A), it was noted that the potential of Ox_1 varied in the range of 0.1–0.225 V. Thus, PEIS responses of a 10 mM $CuSO_4 \cdot 5H_2O$ solution (with 0.1 M KCl as electrolyte) were recorded by applying the DC voltage in the potential range of 0–0.25 V (at an interval of 0.05 V) to determine the voltage at which the kinetics of the redox process is the quickest, as shown in Figure 6.3.

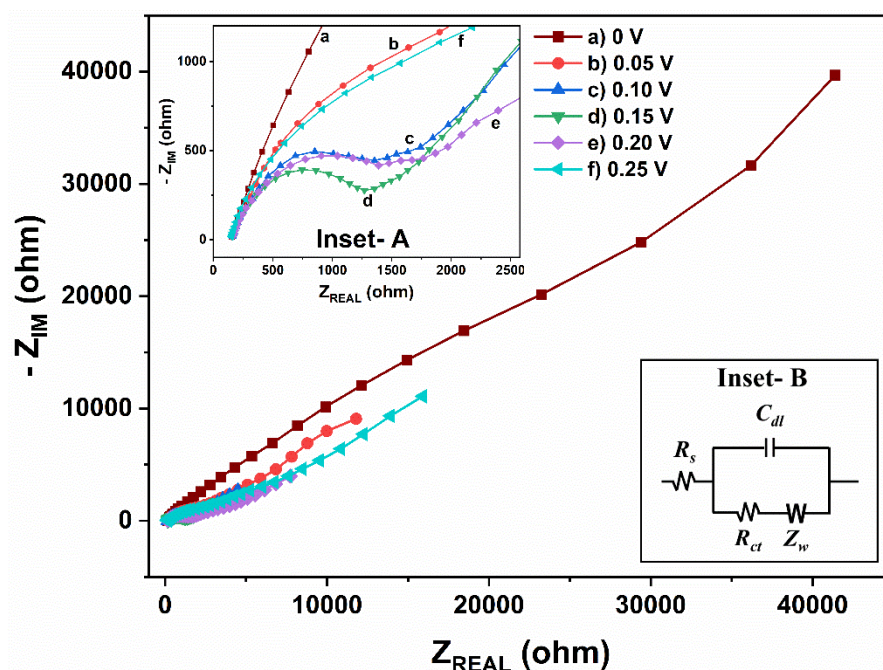


Figure 6.3: PEIS response recorded for copper sulphate solution with the applied DC voltage being a) 0 V, b) 0.05 V, c) 0.10 V, d) 0.15 V, e) 0.20 V and f) 0.25 V. ‘Inset-A’ shows the enlarged impedance spectra for the solutions at higher frequency region and ‘Inset-B’ shows the equivalent circuit model.

From the impedance spectra obtained, it can be stated that the solution resistance (denoted by R_s in the equivalent circuit model) is not affected by the applied DC voltage. However, the other circuit elements like charge transfer resistance (R_{ct}), double layer capacitance (C_{dl}) and Warburg resistance (Z_w) are governed by the applied DC voltage. The magnitude of R_{ct} was noted to be the lowest (represented by the smallest semi-circle) when a DC voltage of 0.15 V was applied, as can be comprehended from curve ‘d’. For two of its neighbouring DC voltages (0.10 V and 0.20 V), the R_{ct} magnitude increased moderately, as indicated by curve ‘c’ and curve ‘e’, respectively. On perturbing the system

with comparatively higher or lower DC voltages (0 V, 0.05 and 0.25 V), it can be seen that the R_{ct} magnitude greatly increased, as indicated by curve 'a', curve 'b' and curve 'f', respectively.

Thus, it can be inferred from this study that the redox process is more feasible when a DC voltage of 0.15 V is applied to the 10 mM $\text{CuSO}_4 \cdot 5\text{H}_2\text{O}$ solution system.

6.3.3 Electrochemical study of creatinine-copper interaction in the aqueous medium

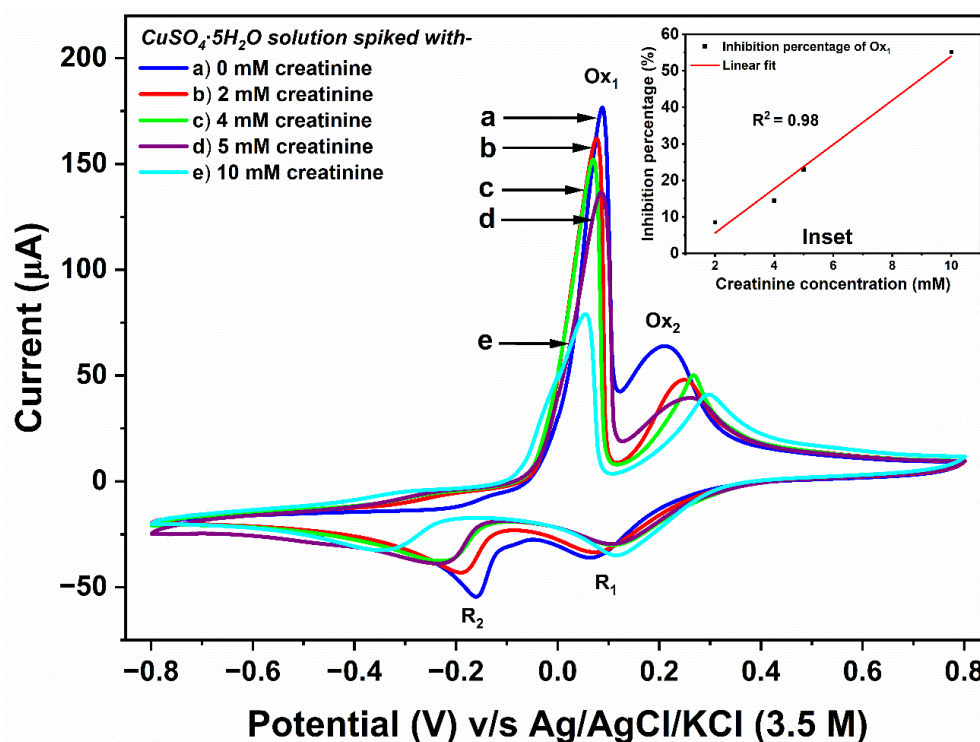
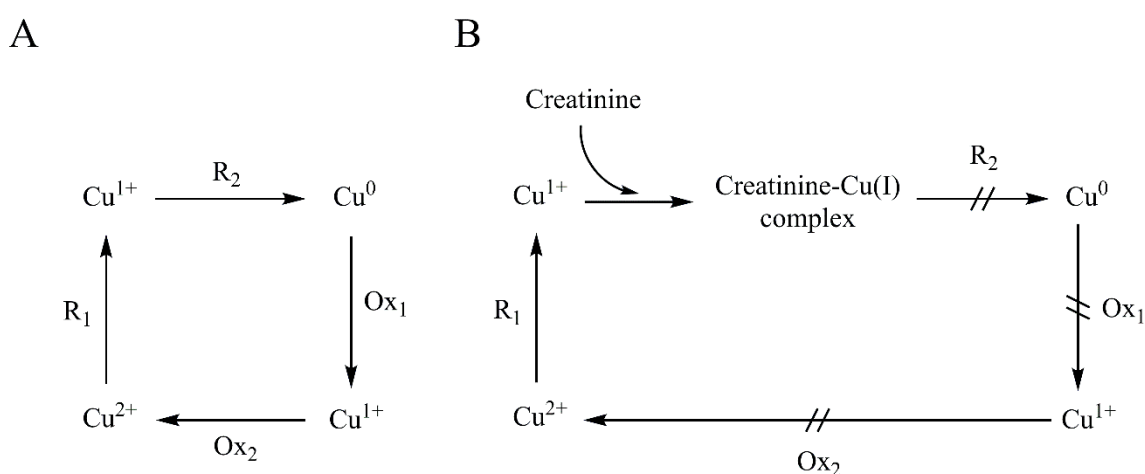


Figure 6.4: Stable CVs (same cycle) obtained for copper sulphate solution spiked with a) 0 mM, b) 2 mM, c) 4 mM, d) 5 mM and e) 10 mM creatinine. 'Inset' shows the plot of percentage inhibition (%) of Ox₁ intensity against the creatinine concentration (mM).

Figure 6.4 shows the CVs recorded for 5 mM $\text{CuSO}_4 \cdot 5\text{H}_2\text{O}$ solution (with 0.1 M KCl as electrolyte) in the absence and presence of different creatinine concentrations. As can be seen in the CVs, the peak, R₁, was not greatly affected in the presence of creatinine. Only slight shifts in the intensity and position of R₁ were noted in the presence of creatinine, which can be attributed to the coordination of creatinine with Cu^{2+} , as commonly reasoned out in the literature. Hence, it can be stated that the creatinine-Cu(II)

complexation occurs only to a small extent in the aqueous medium as the reduction process of Cu^{2+} to Cu^{1+} is slightly affected. However, considerable inhibition of the intensities of other peaks (R_2 , Ox_1 and Ox_2) was observed. These observations indicate the coordination of creatinine dominantly with Cu^{1+} ions. Owing to the creatinine- $\text{Cu}(\text{I})$ complexation, the concentration of free Cu^{1+} ions available in the system decreases. Thus, a decrease in the intensity of R_2 was observed in the presence of creatinine. Consequently, the concentration of Cu^0 decreases in the system, which further leads to the decrease of Ox_1 and Ox_2 intensity, as explained in Scheme 6.1.



Scheme 6.1: A) Redox processes occurring in the copper sulphate solution, and B) Inhibition of the redox processes in the presence of creatinine.

Due to the lower intensities of R_2 and Ox_2 , even in the absence of creatinine, the further decrease in these intensities was seemingly irregular in the presence of creatinine. However, the decrease in the intensity of the major peak, Ox_1 , was found to be linear with the creatinine concentrations. The 'inset' in Figure 6.4 shows a linear increase ($R^2 = 0.98$) of the inhibition percentage of Ox_1 with creatinine concentrations.

While the complexation of creatinine with both Cu^{2+} and Cu^{1+} ions has been proven in the literature, this study reveals that creatinine majorly coordinates with Cu^{1+} ions in the aqueous medium and coordination with Cu^{2+} ions possibly occurs to a much smaller extent.

6.3.4 Spectroscopic analysis of creatinine-copper interaction

Creatine- Cu^{2+} interaction was studied in the PBS medium as Cu(II) salts are highly water soluble. However, Cu(I) salts have poor solubility in water medium, but these salts dissolve in liquid ammonia and acetonitrile [17–19]. Thus, creatinine- Cu^{1+} interaction was studied in 1:1 acetonitrile-water medium. The baselines were accordingly adjusted to record the respective spectra.

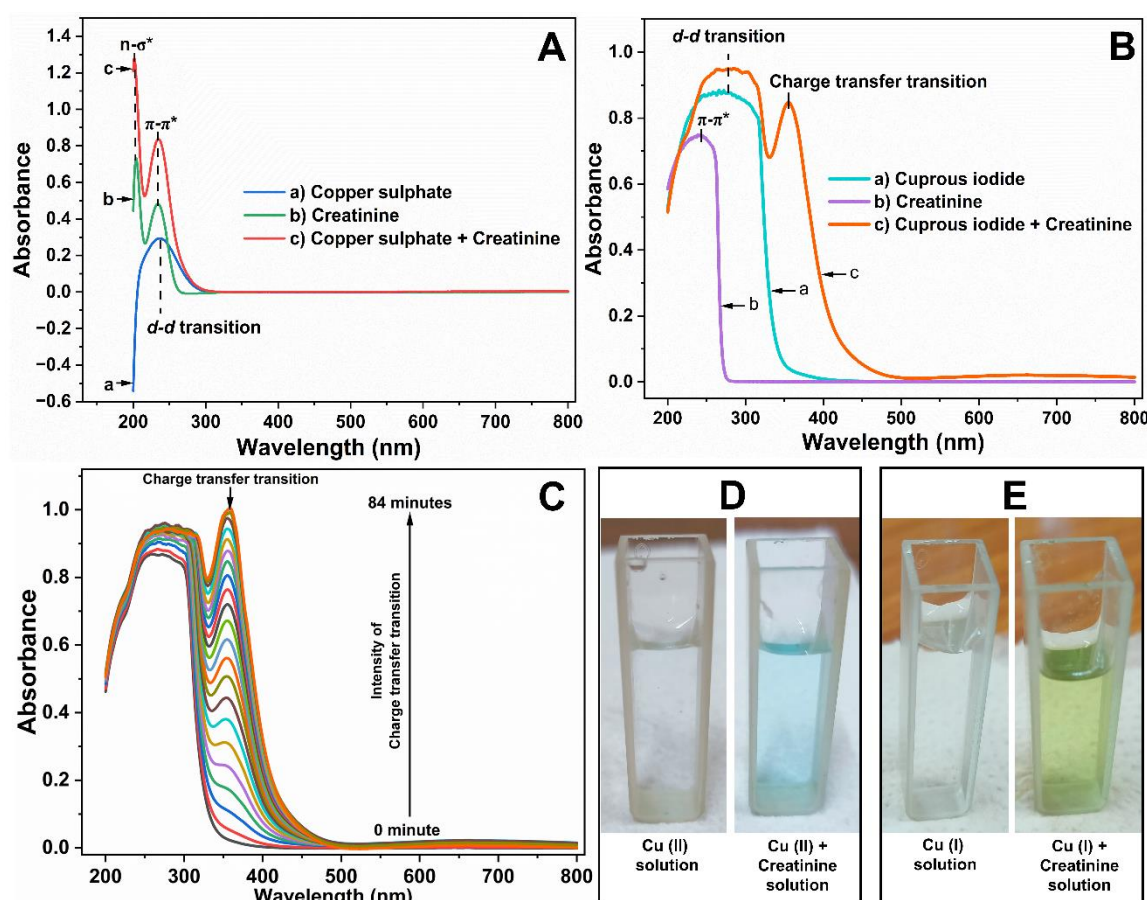


Figure 6.5: UV-vis spectra of: A) PBS solution containing (a) 0.1 mM copper sulphate, (b) 0.1 mM creatinine, and (c) isomolar copper sulphate and creatinine; B) 1:1 acetonitrile-water solution containing (a) 5 mM cuprous iodide, (b) 5 mM creatinine, and (c) isomolar cuprous iodide and creatinine; and C) isomolar cuprous iodide-creatinine solution recorded at a time interval of 4 minutes unto 84 minutes. 'D' and 'E' show the colour change on adding creatinine in solutions containing Cu^{2+} and Cu^{1+} ions respectively.

The recorded UV-vis spectra of a 0.1 mM $\text{CuSO}_4 \cdot 5\text{H}_2\text{O}$ solution, a 0.1 mM CRS and their mixture are shown in Figure 6.5 (A). In the spectrum of $\text{CuSO}_4 \cdot 5\text{H}_2\text{O}$ (spectrum a), a broad band around 236 nm was observed which can be assigned to the $d-d$ transition

in the metal ion [20]. In the spectrum of creatinine (spectrum b), bands at 203 nm and 233 nm were observed, which can be assigned to the $n-\sigma^*$ transition in the amine group and $\pi-\pi^*$ transition in the $C=O$ group [21]. These $n-\sigma^*$ and $\pi-\pi^*$ transitions were also observed with enhanced intensity in the spectrum of the solution containing both creatinine and Cu^{2+} (spectrum c). The hyperchromic effect, thus noted in spectrum 'c', can be attributed to the coordination of Cu^{2+} ions with the secondary amine group of creatinine, which also acts as an auxochrome. Thus, the UV-vis analysis implies the coordination of creatinine and Cu^{2+} ions.

The recorded UV-vis spectra of a 5 mM CuI solution, a 5 mM CRS and their mixture are shown in Figure 6.5 (B). A broad band was observed at 278 nm in the spectrum of CuI (spectrum a) which can be attributed to the $d-d$ transition in the metal ion [22]. In the spectrum of creatinine (spectrum b), the expected $\pi-\pi^*$ transition for the $C=O$ group was observed at 243 nm. However, in the spectrum of the solution containing both CuI and creatinine (spectrum c), a new peak at 355 nm was observed, which inferred the formation of the creatinine-Cu(I) complex and can be attributed to the charge transfer transition. Furthermore, a hyperchromic shift in the $d-d$ transition was also observed due to the complexation.

It must be noted that, unlike the creatinine- Cu^{2+} solution spectrum, the spectrum of the solution containing creatinine- Cu^{1+} demonstrated a time-dependent variation, as shown in Figure 6.5 (C). As the spectra were recorded after different mixing times, it was observed that the intensity of the spectral band due to charge transfer transition initially increased with time, followed by saturation after 80 minutes. A correlation exists between these spectroscopic responses and the visual colour changes observed in the creatinine-cobalt solutions. The addition of creatinine to a solution containing Cu^{2+} ions immediately deepened the faint blue colour of the latter and persisted thereafter, as shown in Figure 6.5 (D). On the other hand, as shown in Figure 6.5 (E), the addition of creatinine to a colourless solution containing Cu^{1+} ions turned the latter into yellowish-green, while gradually intensifying the colour.

From these spectroscopic findings, which confirmed creatinine coordination with Cu^{2+} and Cu^{1+} , it can be stated that the creatinine- Cu^{1+} complexation occurs steadily over a longer period of time, compared to creatinine- Cu^{2+} complexation.

6.3.5 Chronoamperometry response to fabricate the Cu⁰/Pt electrode

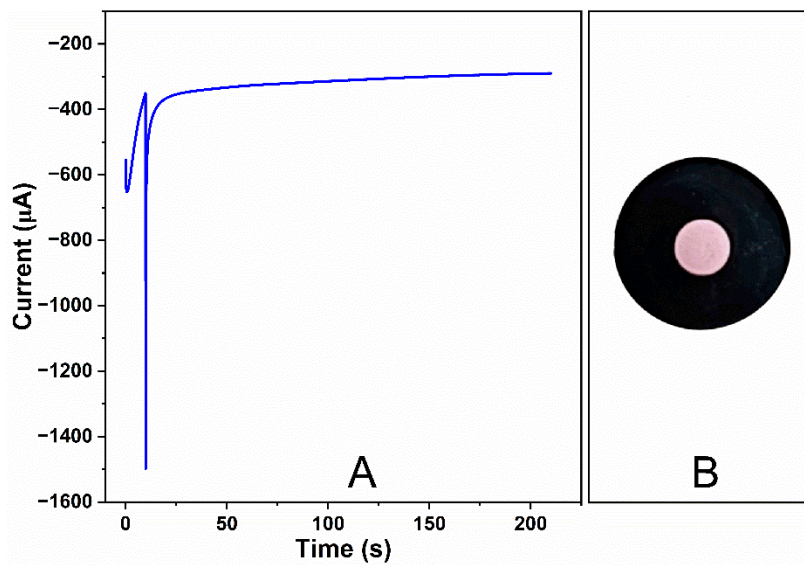


Figure 6.6: A) CA response of acidic copper sulphate solution at the constant potential of -0.2 V. B) Pt electrode surface modified with reddish-brown deposition of Cu^0 .

Figure 6.6 shows the CA response of the acidic 1 mM $\text{CuSO}_4 \cdot 5\text{H}_2\text{O}$ solution. By holding the potential initially at 0.3 V for 10 s, the presence of only Cu^{2+} ions was ensured in the system. Then, as the potential was stepped to -0.2 V, a sharp peak was obtained, due to the capacitive current and also due to the reduction of the Cu^{2+} ions on the electrode surface to deposit Cu^0 . As expected, the currents decay with time. After the electrochemical operation, a reddish-brown deposition of Cu^0 on the electrode surface was obtained, as shown in Figure 6.6 (B).

6.3.6 Electrochemical (DPV) analysis with Cu⁰/Pt electrode and the effect of consecutive DPV runs

The Cu^0/Pt electrode was used to record the CV and DPV of PBS and CRS, as shown in Figure 6.7. In the CV of PBS, as can be seen in curve 'a' in Figure 6.7 (A), an oxidation peak, Ox_1 , was observed which can be attributed to the oxidation of Cu^0 on the electrode surface to Cu^{1+} . However, the peak appeared broad and seemingly merged with the oxidation peak due to the oxidation of Cu^{1+} to Cu^{2+} . In the same voltammogram, two reduction peaks were also observed as expected. All these peaks appeared at slightly shifted potentials, compared to their corresponding potentials in the voltammograms of

aqueous $\text{CuSO}_4 \cdot 5\text{H}_2\text{O}$ solution. This potential shift can be attributed to the medium (PBS) effect.

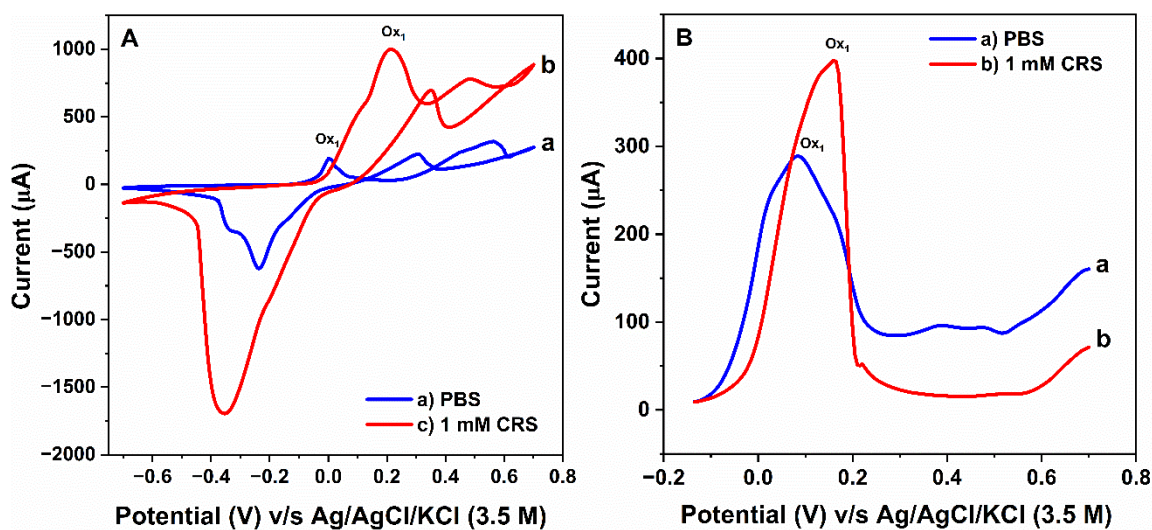


Figure 6.7: CV (A) and DPV (B) obtained for a) PBS and b) CRS with Cu^0/Pt electrode.

In the CV of CRS, as can be seen in curve 'b' in Figure 6.7 (A), the intensity of Ox_1 enormously increased. This increase in intensity in the presence of creatinine can be attributed to the strong affinity of creatinine to coordinate with Cu^{1+} ions. Thus, an increase in the oxidation of Cu^0 to Cu^{1+} was observed. The Ox_1 peak in CRS appeared much broader, which also apparently masked the peak for oxidation of Cu^{1+} to Cu^{2+} . Simultaneously, an immense increase in the intensity of the reduction peaks was also observed. However, unlike in the voltammogram of PBS, the reduction peaks in the voltammogram of CRS appeared to have merged.

Multiple crossings between the anodic and cathodic parts were observed in the voltammograms at the higher potential region. Such unusual voltammogram crossings were also reported at different potentials while accomplishing electrodeposition of copper [23-25], cobalt [26] and silver [27] on different electrode surfaces. Although the exact origin of such a phenomenon is not very clear, it can be attributed to the structural reformation at the electrode surface. *Emery et al.* [25] emphasized that the voltammogram crossings are not a feature of direct deposition but are expected when 3-D nucleation of the deposited species occurs on the electrode surfaces.

DPVs were recorded, as shown in Figure 6.7 (B), to obtain the oxidation peaks. The voltammograms exhibited responses similar to those of their corresponding CV. Broad peaks for Ox₁ were observed, with its intensity in CRS higher than in the PBS. Despite the better sensitivity of the DPV technique, the second expected oxidation peak (for Cu¹⁺ to Cu²⁺) couldn't be resolved.

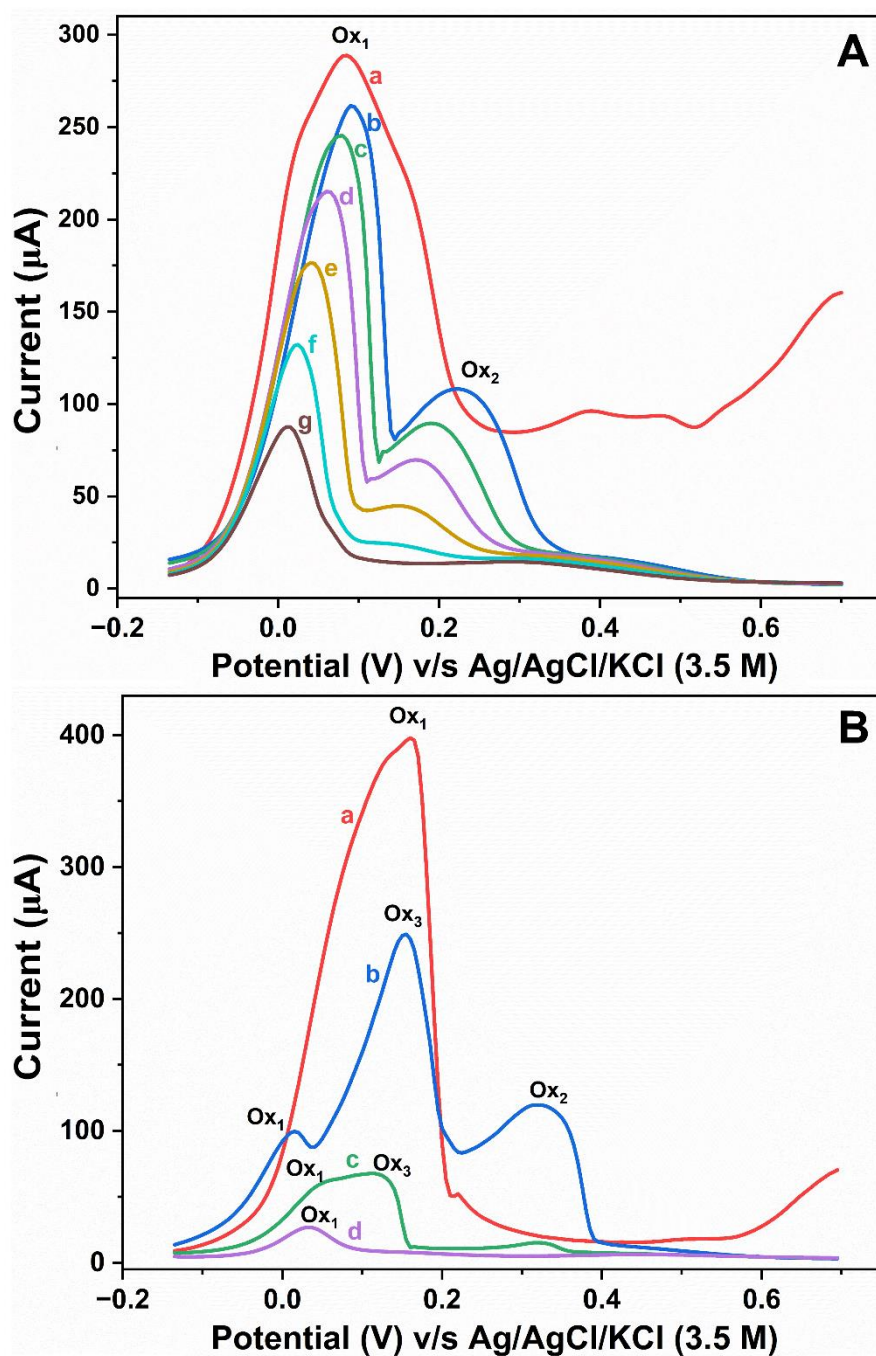


Figure 6.8: Successive DPV runs with Cu⁰/Pt electrode in (A) PBS (a–g) and (B) CRS (a–d).

Successive DPVs were recorded for PBS and CRS Cu⁰/Pt electrode as shown in Figure 6.8. With every successive DPV run, degradation in the intensity of the oxidation peaks was observed due to the stripping of the Cu⁰ species from the electrode surface. This observation infers poor reusability of the Cu⁰/Pt electrode. The intensity degradation in CRS was much quicker than in PBS. Thus, it was noted that if the DPV of the first runs are compared, then the oxidation peak in the presence of creatinine exhibits higher intensity than in the absence of creatinine. From the subsequent DPV runs, the intensity in the absence of creatinine appears higher than in the presence of creatinine. The cause of the quicker degradation of the peak in the presence of creatinine and some other interesting observations marked from the reusability test are explained below.

As can be seen in the successive DPVs in PBS in Figure 6.8 (A), the oxidation peak, Ox₁, narrowed from the 2nd run (due to the lower concentration of Cu⁰ on the electrode surface) and simultaneously, the second oxidation peak, Ox₂, for Cu¹⁺/Cu²⁺ was obtained. Both the degrading peaks displayed a slight shift towards the negative potential with each run.

The presence of creatinine in the system facilitates more oxidation of Cu⁰ from the surface; hence, the concentration of Cu⁰ on the electrode surface is likely to decrease considerably after the first run. This is reflected by the low intensity of Ox₁ in the second DPV run in CRS, as shown by curve 'b' in Figure 6.8 (B). This also explains the quicker degradation of the oxidation peak in CRS compared to PBS. Furthermore, as observed in the successive DPVs of PBS, Ox₂ was resolved from the second run in the DPV of CRS. The most interesting observation in the second DPV run in CRS was the appearance of another oxidation peak, Ox₃, which wasn't obtained in the DPV of PBS. As peak positions are expected to vary for the oxidation of a free redox centre and a coordinated redox centre, Ox₃ can be possibly attributed to the oxidation of the creatinine-Cu(I) complex to the creatinine-Cu(II) complex. The intensity of all three oxidation peaks in CRS further degraded in the subsequent runs.

6.3.7 Chronopotentiometry response for fabrication of TIP/Pt

The CP responses for the fabrication of TIP/Pt and PPy/Pt electrodes are shown by curves 'a' and 'b', respectively, in Figure 6.9.

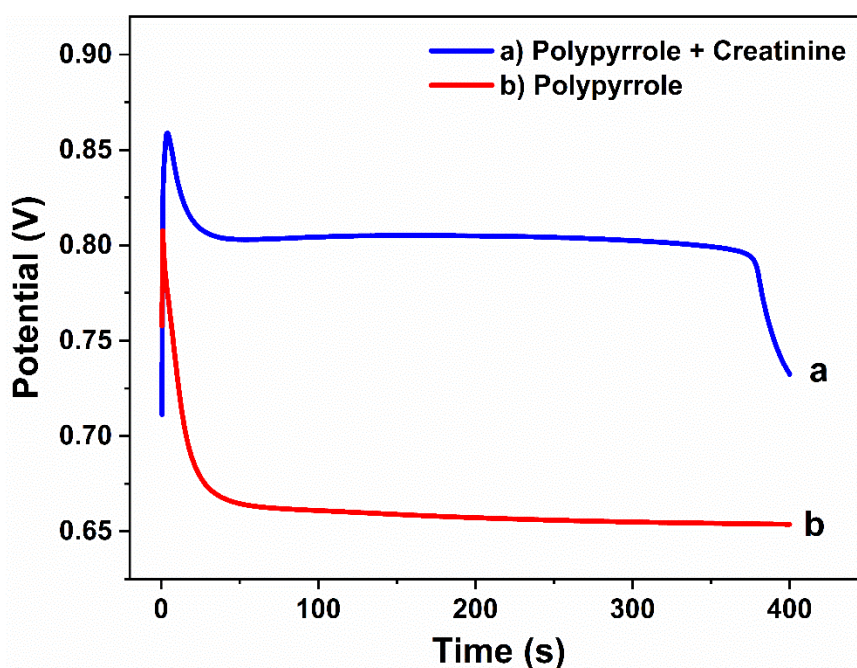


Figure 6.9: CP responses of 0.1 M KNO₃ solution containing a) 100 mM pyrrole monomer with 30 mM creatinine, and b) 100 mM pyrrole monomer.

When CP (curve b) was recorded for 0.1 M KNO₃ solution containing 100 mM pyrrole monomer, one sudden potential change was observed in the response, which occurred to commence the pyrrole monomer reflux towards the electrode. Then, as the system maintained a potential of approximately 0.66 V (with a sluggish declination with time), the pyrrole monomers were oxidized on the electrode surface to supply the constant current. Meanwhile, polymerization also occurred to yield the PPy/Pt electrode.

However, when CP (curve a) was recorded for 0.1 M KNO₃ solution containing 100 mM pyrrole monomer and 30 mM creatinine, two sudden potential changes were observed in the response. The first potential change possibly commences the reflux of the pyrrole monomers, weakly and non-covalently bonded with creatinine molecules. Hence, a higher potential (compared to curve 'b') of approximately 0.80 V was maintained for some time, at which the creatinine-bound pyrrole monomers were oxidized. After 370 s, another potential change was observed which marked the cessation of the oxidation of creatinine-bound pyrrole monomers and the commencement of the free pyrrole monomer reflux. Meanwhile, polymerization also occurred to yield the TIP/Pt electrode.

The TIP/Pt electrode exhibited a brown deposition on the electrode surface.

6.3.8 Spectroscopic analysis of creatinine-pyrrole interaction

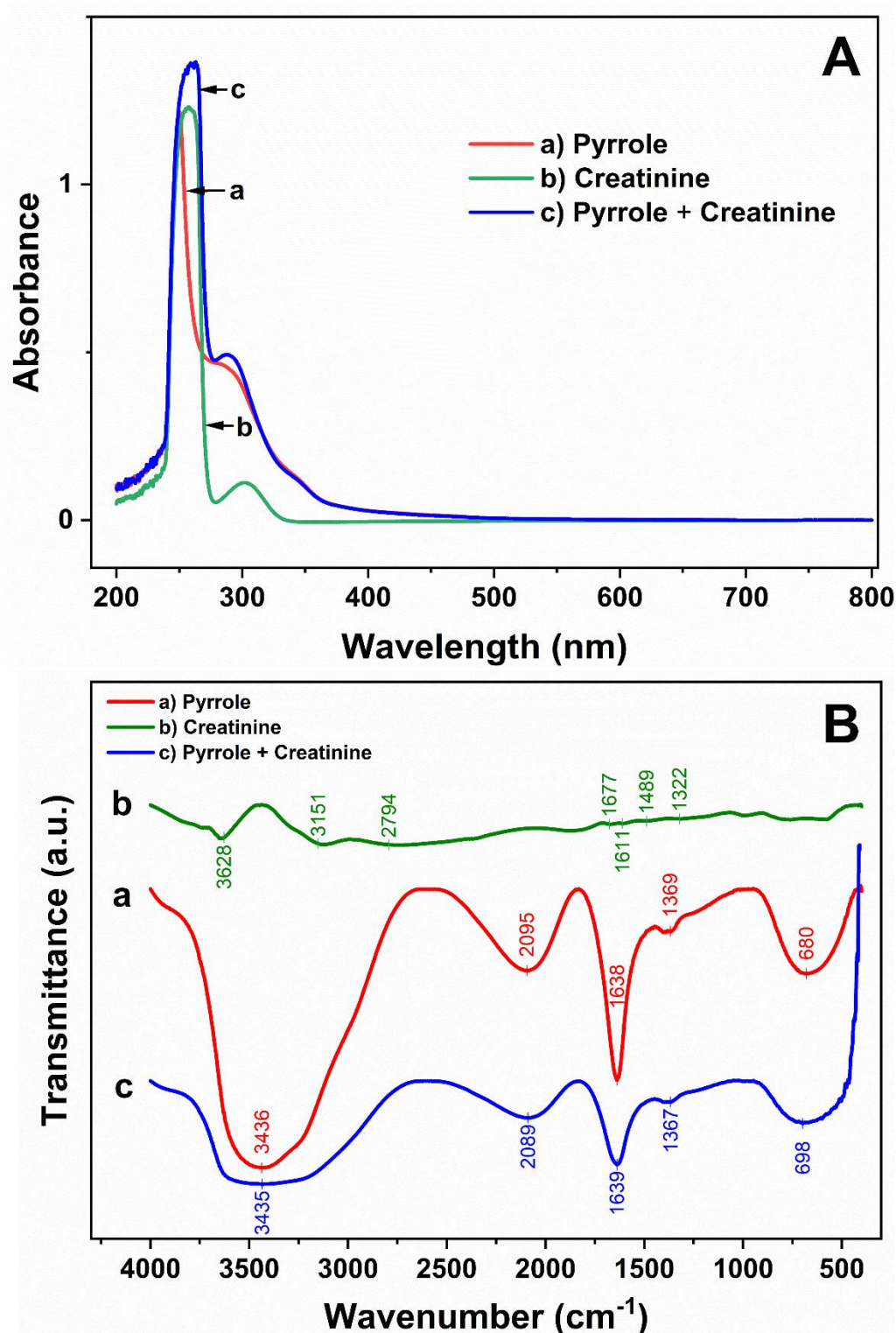


Figure 6.10: UV-vis spectra (A) and FTIR spectra (B) of 0.1 M KNO_3 solution containing a) 10 mM pyrrole monomer, b) 3 mM creatinine and c) 10 mM pyrrole monomer with 3 mM creatinine.

As a weak non-covalent interaction between pyrrole and creatinine has been proposed in the previous section, spectroscopic evidence was also gathered to confirm the interaction. The UV-vis and FTIR spectra recorded for a 10 mM pyrrole monomer solution, a 3 mM creatinine solution and their mixture, are shown in Figure 6.10 (A) and Figure 6.10 (B) respectively. As the solutions were prepared in 0.1 M KNO₃ the baseline was adjusted accordingly to record the UV-vis spectra and the solvent spectrum was subtracted to obtain the required FTIR spectra.

6.3.8.1 UV-vis analysis

The UV-vis spectra in Figure 6.10 (A) were analyzed. Absorption bands were observed at 250 nm and 287 nm in the spectrum of pyrrole (spectrum a), which can be attributed to the π - π^* transition in the C = C chromophore [28, 29]. A high-intensity band at 257 nm and a low-intensity band at 302 nm were observed in the spectrum of creatinine (spectrum b), which can be ascribed to the π - π^* transition and the n- π^* transition in the carbonyl group, respectively [21]. In the spectrum of the solution containing both pyrrole and creatinine (spectrum c), a broad band at 261 nm was observed where the π - π^* transitions occurring in the carbonyl group of creatinine and in C = C of pyrrole, were seemingly merged. Another band at 289 nm was observed due to the π - π^* transition in C = C of pyrrole. As the n- π^* transition in the carbonyl group of creatinine is a low-intensity forbidden transition [21], it stayed masked in spectrum 'c'. However, hyperchromic effects were observed in the π - π^* transitions in spectrum 'c', compared to the native bands in spectra 'a' and 'b'. The hyperchromic effect in the π - π^* transition occurring in the carbonyl group of creatinine can be attributed to the structural change in the auxochrome (secondary amine group) adjacent to the carbonyl group, due to a weak interaction (like H-bonding) with pyrrole. This also explains the hyperchromic effect observed in the π - π^* transitions occurring in C = C of pyrrole.

6.3.8.2 FTIR analysis

The FTIR spectra in Figure 6.10 (B) were analyzed. In the spectrum of pyrrole (spectrum a), the characteristic band for N-H stretching in the secondary amine group was observed at 3436 cm⁻¹, the C = C stretching frequency was observed at 1638 cm⁻¹ and C-N stretching frequency at 1369 cm⁻¹ [21]. While the band at the lower frequency (680 cm⁻¹) region can be ascribed to C-H bending, the band at 2095 cm⁻¹ can be attributed to C

= C overtones [21]. In the spectrum of creatinine (spectrum b), the peaks at 3628 cm^{-1} and 3151 cm^{-1} can be attributed to the N-H stretching in the primary amine group and the C-H stretching frequency was observed at 2794 cm^{-1} [21, 30]. While the peak at 1677 cm^{-1} can be ascribed to C = O stretching under resonance effect, the peak at 1611 cm^{-1} can be attributed to the C-N stretching frequency and the peaks at 1489 cm^{-1} and 1322 cm^{-1} can be attributed to the bending of methyl and methylene groups [30]. All the characteristic peaks of pyrrole were also observed in the spectrum of the solution containing pyrrole and creatinine (spectrum c). However, in the presence of creatinine, a broadening of the N-H stretching band of pyrrole was observed in spectrum 'c', which also inferred the H-bonding interaction between creatinine and pyrrole monomer.

Thus, UV-vis and FTIR analyses confirmed the non-covalent interaction between pyrrole and creatinine.

6.3.9 CIP/Pt formation and validation

It is easier to overcome the weak non-covalent interaction between the monomeric units and template molecules via simple extraction techniques to fabricate molecularly imprinted polymers (MIPs) [31]. As creatinine is readily soluble in water and polypyrrole strongly adhered to the electrode surface, the CIP/Pt electrode was formed by dipping the surface of TIP/Pt in distilled water with continuous stirring for half an hour to overcome the weak non-covalent creatinine-pyrrole interaction.

SEM images of the MIP electrode materials were recorded, as shown in Figure 6.11, to note their morphological differences. Some densely packed globular agglomerates were observed in the SEM image of the polypyrrole film [Figure 6.11 (a) and 6.11 (d)], which is in agreement with existing literature [32]. In the SEM image of the co-deposited creatinine and polypyrrole film [Figure 6.11 (b) and 6.11 (e)], some multi-layered structures with concave, ovoid cavities, atop the glomerular agglomerates of polypyrrole, were observed. The concave structures possibly represented creatinine, bound non-covalently to the polypyrrole matrix, as these structures were not observed in the SEM image of the creatinine-imprinted polypyrrole (CIP) film [Figure 6.11 (c) and 6.11 (f)]. The SEM image of the CIP film revealed globular agglomerates that were relatively loosely packed and smaller in size compared to those observed in the SEM image of the polypyrrole film. While similar morphological shapes of imprinted and non-imprinted

polymers are often reported in the literature [33, 34], the decrease in the agglomerate size and density in our CIP film inferred that polymerization of the pyrrole monomers was impeded during the co-deposition step, thereby facilitating the accommodation of creatinine molecules within the material. Thus, more free spaces were located in the CIP film formed after creatinine removal, apart from some dented areas in the agglomerates, possibly corresponding to the creatinine binding sites. Hence, these findings supported the formation of the CIP/Pt.

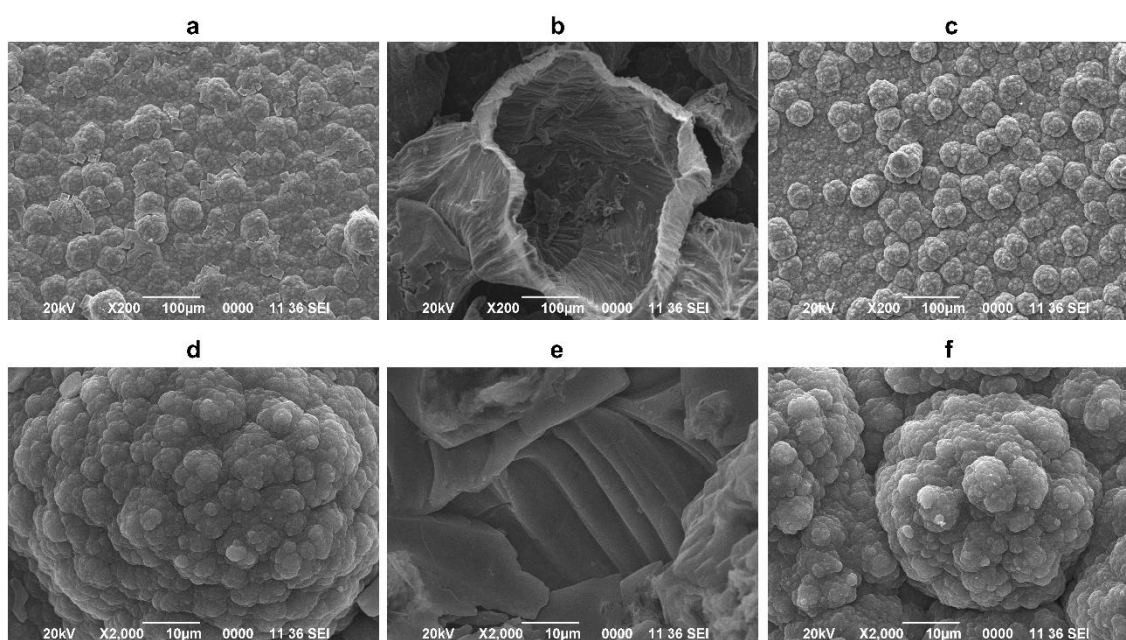


Figure 6.11: SEM images of a) polypyrrole film, b) co-deposited creatinine and polypyrrole film, and c) creatinine-imprinted polypyrrole film. 'd', 'e' and 'f' are the respective SEM images at higher magnification.

Furthermore, an innovative approach was undertaken to support the successful formation of the CIP/Pt electrode by carrying out some electrochemical analyses.

CVs were recorded for 5 mM $\text{CuSO}_4 \cdot 5\text{H}_2\text{O}$ solution (with 0.1 M KCl as electrolyte), with the TIP/Pt electrode (curve a) and the CIP/Pt electrode (curve b), as shown in Figure 6.12. In the voltammogram recorded with the TIP/Pt electrode, no redox peak for copper was obtained, as seen in curve 'a'. In contrast, the expected four redox peaks of copper were obtained, with the CIP/Pt electrode, as seen in curve 'b'. These observations indicated that the creatinine molecules present on the surface of the TIP/Pt

electrode coordinated with the Cu^{2+} ions and inhibited the redox processes of the copper ions. However, the appearance of the redox peaks of copper with the CIP/Pt electrode suggested the removal of the creatinine molecules from the electrode surface, thereby proving the existence of an MIP framework as well as creatinine-copper interaction.

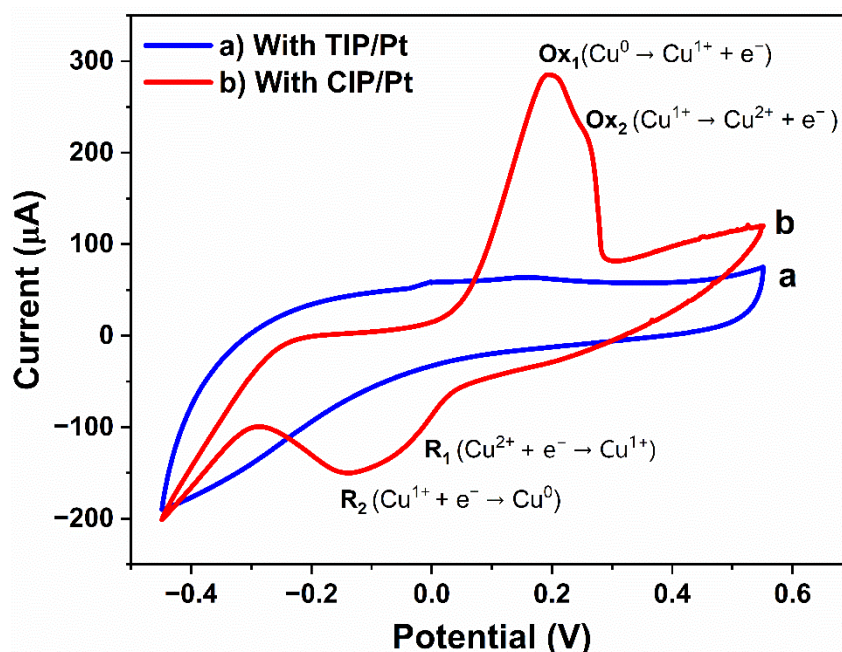


Figure 6.12: CVs recorded for copper sulphate solution with a) TIP/Pt and b) CIP/Pt electrode.

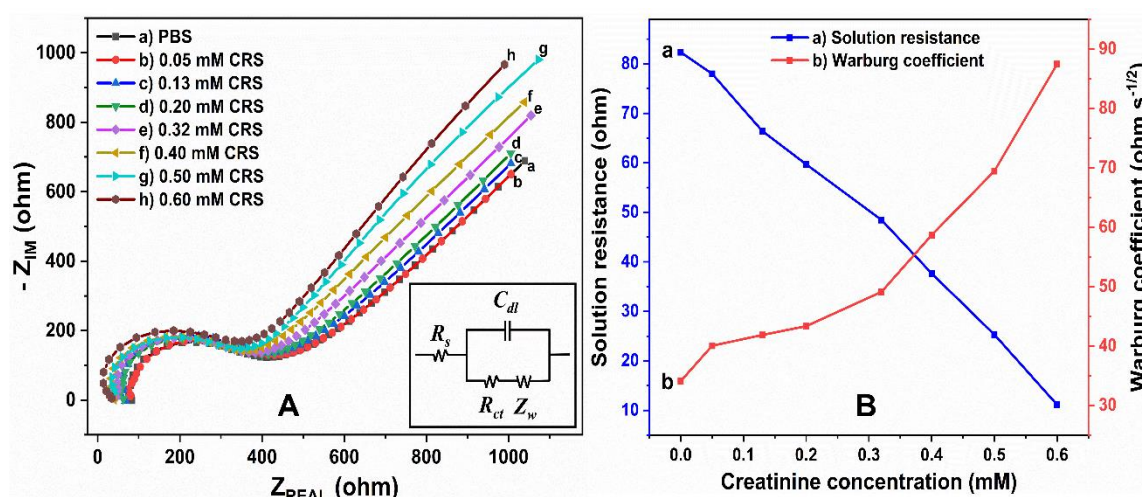


Figure 6.13: A) GEIS responses recorded in PBS (a) and in different concentrations of CRS (b–h) with CIP/Pt electrode. B) Variation of solution resistance (a) and Warburg coefficient (b) with creatinine concentration. The inset in 'A' shows the equivalent circuit model.

GEIS responses were also recorded with CIP/Pt electrode for CRS by varying the creatinine concentration from 0.05 M to 0.60 mM, as shown in Figure 6.13 (A). As creatinine is electrochemically inactive, only the redox processes of the deposited polypyrrole are possible due to the perturbation effect while recording the GEIS responses. Hence, the values for charge transfer resistance (R_{ct}) were very close, as can be contemplated by the dimension of the semi-circles in Figure 6.13 (A). However, it was noted that with the increase in creatinine concentration, there was an increase in the Warburg impedance (Z_w) and a decrease in the solution resistance (R_s). These phenomena also inferred the successful fabrication of the CIP/Pt electrode.

With increased creatinine concentration, more creatinine molecules are expected to diffuse towards the recognition centres on the modified electrode surface. Thus, an increase in the Warburg impedance with creatinine concentration was observed. The higher diffusion of the electrochemically inactive creatinine molecules in the solution, with higher concentration, may also be allied with the decrease in the solution resistance. The decrease in the solution resistance and increase in the Warburg coefficient with the increase in creatinine concentration are graphically represented in Figure 6.13 (B).

The values obtained for all the circuit elements have been presented in Table 6.1.

Table 6.1: Values calculated for solution resistance (R_s), charge transfer resistance (R_{ct}) capacitance (C_{dl}) and Warburg coefficient (σ) from the fitted GEIS curves obtained for different concentrations of creatinine solution, with CIP/Pt electrode.

Concentration of creatinine (mM)	R_s (Ohm)	C_{dl} (F)	R_{ct} (Ohm)	σ (ohm s ^{-1/2})
0	82.34	2.226×10^{-9}	311.40	34.088
0.05	77.97	2.377×10^{-9}	319.90	40.049
0.13	66.42	2.208×10^{-9}	314.60	41.851
0.20	59.70	2.177×10^{-9}	318.60	43.338

0.32	48.46	2.077×10^{-9}	308.80	49.124
0.40	37.66	2.374×10^{-9}	320.20	58.686
0.50	25.30	2.444×10^{-9}	314.20	69.449
0.60	11.13	2.228×10^{-9}	319.78	87.457

6.4 Conclusion

In this chapter, the electrochemical response of copper has been characterized using voltammetry and PEIS. Selecting a well-resolved voltammogram with correctly assigned redox peaks of copper enabled us to understand the creatinine-copper interaction properly during the electrochemical processes. It has been established through this electrochemical study that creatinine reacts majorly with Cu^{1+} in the aqueous medium and coordination with Cu^{2+} ions occurs to a much smaller extent, evidenced by significant inhibition in the $\text{Cu}^{1+}/\text{Cu}^0$ reduction in the presence of creatinine. UV-vis spectroscopic study corroborated this finding. While a new charge transfer peak with a time-dependent increase in absorption was seen in the case of creatinine-Cu(I) reaction, only a hyperchromic shift was seen in the case of creatinine-Cu(II). When a Cu^0 deposited electrode was used to record the voltammograms of creatinine solution, the greater affinity of creatinine coordination with Cu^{1+} caused the increase in the intensity of the $\text{Cu}^0/\text{Cu}^{1+}$ oxidation peak in the first voltammogram run, followed by quicker degradation in its intensity from the subsequent runs, thus, indicating that creatinine catalyzes the electrochemical oxidation. Creatinine interaction with polypyrrole was studied with UV-vis and FTIR spectroscopy, which revealed a weak non-covalent interaction between the two. This has led to the successful fabrication of an MIP platform for creatinine sensing with polypyrrole as the host matrix. SEM analysis revealed the loosely held globular agglomerates of the MIP with creatinine binding sites. Furthermore, the successful fabrication of the sensing platform was further verified with two different electrochemical approaches. In the first approach, creatinine-copper electrochemical interaction was utilized as creatinine-impregnated polypyrrole blocks the redox peak of copper on the Pt surface. In the second approach, GEIS responses of creatinine solutions were analyzed. GEIS responses recorded with the MIP-electrode

showed an increase in the Warburg resistance and a decrease in solution resistance with creatinine concentration. The MIP platform serves as a base that can be further optimized and refined to create a practical, real-world creatinine sensing device.

References

- [1] Raveendran, J., Resmi, P. E., Ramachandran, T., Nair, B. G. and Babu, T. S. Fabrication of a disposable non-enzymatic electrochemical creatinine sensor. *Sensors and Actuators B: Chemical*, 243:589–595, 2017.
- [2] Sato, N., Takeda, K. and Nakamura, N. Development of a Copper-electrodeposited Gold Electrode for an Amperometric Creatinine Sensor to Detect Creatinine in Urine without Pretreatment. *Electrochemistry*, 89(3):313–316, 2021.
- [3] Jankhunthod, S., Kaewket, K., Termsombut, P., Khamdang, C. and Ngamchuea, K. Electrodeposited copper nanoparticles for creatinine detection via the in situ formation of copper-creatinine complexes. *Analytical and Bioanalytical Chemistry*, 415(16):3231–3242, 2023.
- [4] Kaewket, K. and Ngamchuea, K. Electrochemical detection of creatinine: exploiting copper (ii) complexes at Pt microelectrode arrays. *RSC Advances*, 13(47):33210–33220, 2023.
- [5] Udupa, M. R. and Krebs, B. Crystal and molecular structure of creatinium tetrachlorocuprate (II). *Inorganica Chimica Acta*, 33:241–244, 1979.
- [6] Mitewa, M., Bontchev, P. R. and Kabassanov, K. A four-membered chelate complex of Cu (II) with creatinine. *Polyhedron*, 4(7):1159–1161, 1985.
- [7] Mitewa, M., Gencheva, G., Ivanova, I., Zhecheva, E. and Mechandjiev, D. Complex formation of monomeric and dimeric copper (II) complexes with creatinine in organic media. *Polyhedron*, 10(15):1767–1771, 1991.
- [8] Kalasin, S., Sangnuang, P., Khownarumit, P., Tang, I. M. and Surareungchai, W. Evidence of Cu (I) coupling with creatinine using cuprous nanoparticles encapsulated with polyacrylic acid gel-Cu (II) in facilitating the determination of advanced kidney dysfunctions. *ACS Biomaterials Science & Engineering*, 6(2):1247–1258, 2020.

-
- [9] Prabhu, S. N., Mukhopadhyay, S. C., Gooneratne, C. P., Davidson, A. S. and Liu, G. Molecularly Imprinted Polymer-based detection of creatinine towards smart sensing. *Medical Devices & Sensors*, 3(6):e10133, 2020.
- [10] Khadro, B., Sanglar, C., Bonhomme, A., Errachid, A. and Jaffrezic-Renault, N. Molecularly imprinted polymers (MIP) based electrochemical sensor for detection of urea and creatinine. *Procedia Engineering*, 5:371–374, 2010.
- [11] Prabhu, S. N., Gooneratne, C. P. and Mukhopadhyay, S. C. Development of MEMS sensor for detection of creatinine using MIP based approach—a tutorial paper. *IEEE Sensors Journal*, 21(20):22170–22181, 2021.
- [12] Fall, M., Diagne, A. A., Guene, M., Della Volpe, C., Bonora, P. L., Deflorian, F. and Rossi, S. R. Electrochemical properties and electrochemical impedance spectroscopy of polypyrrole-coated platinum electrodes. *Bulletin of the Chemical Society of Ethiopia*, 20(2):279–293, 2006.
- [13] Wang, D., Haque, S., Williams, T., Karim, F., Hariharalakshmanan, R. K., Al-Mayalee, K. H. and Karabacak, T. Cyclic voltammetry and specific capacitance studies of copper oxide nanostructures grown by hot water treatment. *MRS Advances*, 9:979–985, 2024.
- [14] Amayreh, M., Hourani, W. and Hourani, M. K. Anodic Stripping Voltammetric Determination of Copper in Multivitamin-Mineral Formulations using Iodine-Coated Platinum Electrode. *Methods & Objects of Chemical Analysis*, 16(1):48–56, 2021.
- [15] Trnkova, L., Zerzankova, L., Dycka, F., Mikelova, R. and Jelen, F. Study of copper and purine-copper complexes on modified carbon electrodes by cyclic and elimination voltammetry. *Sensors*, 8(1):429–444, 2008.
- [16] Rana, M. S., Rahman, M. A. and Alam, A. S. A CV study of copper complexation with guanine using glassy carbon electrode in aqueous medium. *International Scholarly Research Notices*, 2014(1):308382, 2014.

- [17] Pranowo, H. D., Bambang Setiaji, A. H. and Rode, B. M. Cu^+ in liquid ammonia and in water: Intermolecular potential function and Monte Carlo simulation. *The Journal of Physical Chemistry A*, 103(50):11115–11120, 1999.
- [18] Luo, Q., Mackay, R. A. and Babu, S. V. Copper dissolution in aqueous ammonia-containing media during chemical mechanical polishing. *Chemistry of Materials*, 9(10):2101–2106, 1997.
- [19] Barth, E. R., Golz, C., Knorr, M. and Strohmman, C. Crystal structure of di- μ -iodido-bis [bis (acetonitrile- κN) copper (I)]. *Acta Crystallographica Section E: Crystallographic Communications*, 71(11):m189–m190, 2015.
- [20] Padamati, S. K., Vedelaar, T. A., Perona Martínez, F., Nusantara, A. C. and Schirhagl, R. Insight into a Fenton-like reaction using Nanodiamond based relaxometry. *Nanomaterials*, 12(14):2422, 2022.
- [21] Pavia, D. L., Lampman, G. M., Kriz, G. S., and Vyvyan, J. R. *Introduction to spectroscopy*. Cengage Learning, Boston, MA, 2008.
- [22] Byranvand, M. M. and Kharat, A. N. Triangular-like cuprous iodide nanostructures: green and rapid synthesis using sugar beet juice. *Romanian Journal of Biochemistry*, 51(2):101–107, 2014.
- [23] Jaya, S., Rao, T. P. and Rao, G. P. Electrochemical phase formation—I. The electrodeposition of copper on glassy carbon. *Electrochimica Acta*, 31(3):343–348, 1986.
- [24] Emery, S. B., Hubble, J. L. and Roy, D. Voltammetric and amperometric analyses of electrochemical nucleation: electrodeposition of copper on nickel and tantalum. *Journal of Electroanalytical Chemistry*, 568:121–133, 2004.
- [25] Srinivasan, R. and Gopalan, P. Order and disorder in electrochemical deposits of copper on graphite. *Surface Science*, 338(1-3):31–40, 1995.
- [26] Palomar-Pardavé, M., González, I., Soto, A. B. and Arce, E. M. Influence of the coordination sphere on the mechanism of cobalt nucleation onto glassy carbon. *Journal of Electroanalytical Chemistry*, 443(1):125–136, 1998.
- [27] Correia, A. N., Dos Santos, M. C., Machado, S. A. S. and Avaca, L. A. Microgravimetric studies of silver electrocrystallization on polycrystalline gold surfaces. *Journal of Electroanalytical Chemistry*, 547(1):53–59, 2003.

- [28] Cui, Z., Coletta, C., Dazzi, A., Lefrancois, P., Gervais, M., Néron, S. and Remita, S. Radiolytic method as a novel approach for the synthesis of nanostructured conducting polypyrrole. *Langmuir*, 30(46):14086–14094, 2014.
- [29] Kherroub, D. E., Bouhadjar, L. and Boucherdoud, A. Synthesis and characterization of novel conductive copolymer poly [(phenylazepane-2-one)-co-(pyrrole)] with improved solubility and conductivity properties. *Journal of Materials Science*, 56:1827–1841, 2021.
- [30] Hussain, N. and Puzari, P. Deciphering the complexation processes of creatinine-cobalt and creatinine-cobalt-2-nitrobenzaldehyde: Morphological, spectroscopic and electrochemical analysis. *Journal of Molecular Structure*, 1316:139042, 2024.
- [31] Sajini, T. and Mathew, B. A brief overview of molecularly imprinted polymers: Highlighting computational design, nano and photo-responsive imprinting. *Talanta Open*, 4:100072, 2021.
- [32] Dutta, R. R. and Puzari, P. Amperometric biosensing of organophosphate and organocarbamate pesticides utilizing polypyrrole entrapped acetylcholinesterase electrode. *Biosensors and Bioelectronics*, 52:166–172, 2014.
- [33] Kamel, A. H., Amr. A. E. G. E., Abdalla, N. S., El-Naggar, M., Al-Omar, M. A., Alkahtani, H. M. and Sayed, A. Y. Novel solid-state potentiometric sensors using polyaniline (PANI) as a solid-contact transducer for flucarbazon herbicide assessment. *Polymers*, 11(11):1796, 2019.
- [34] Quinto, M. L., Khan, S., Vega-Chacón, J., Mortari, B., Wong, A., Taboada Sotomayor, M. D. P. and Picasso, G. Development and Characterization of a Molecularly Imprinted Polymer for the Selective Removal of Brilliant Green Textile Dye from River and Textile Industry Effluents. *Polymers*, 15(18):3709, 2023.